Elastoplastic analysis of external axial surface cracks in tubes

Z. Tonković[1], I. Skozrit[1]

Summary

Systematic detailed linear and non-linear 3-D finite element analyses have been carried out to determine the stress intensity factors, the *J*-integral and the plastic limit loads for external axial semi-elliptical surface cracks in VVER steam generator tubes under internal pressure. The results for the stress intensity factors are presented in terms of the well-known GE/EPRI influence functions to allow comparisons with some results available in the literature. The plastic limit pressure solutions have been developed on the basis of finite element limit load analyses employing elastic-perfectly plastic material behaviour. Using these solutions, a new analytical approximation of the plastic limit pressure has been developed for a wide range of cracks. The proposed stress intensity factors and analytical approximation of limit pressure provide very useful tools for assessing the integrity of pressurized tubes.

Introduction

Operating experience with VVER steam generators has shown that external axial surface cracks present one of the most common causes of loss of the steam generator tube integrity. An accurate computation of the plastic limit pressure and the fracture response characteristics, such as stress intensity factor (SIF) and *J*-integral of cracked tubes, represent a key for the prediction of structural integrity and reliability of pressurized tubes. In contrast with internal axial semi-elliptical surface cracks [1], a very limited number of studies have been reported in the area dealing with the determination of the SIFs for tubes with external axial semi-elliptical surface cracks [2]. Up to now, there have been no detailed 3-D finite element analyses (FEAs) for a wide range of surface cracks on the outside of a tube.

In some Failure Assessment Diagram methods the limit load of a cracked tube is used to define a parameter L_r, that measures the proximity to plastic collapse [3]. Furthermore, when performing a structural integrity assessment using the R6 procedure [3], the limit load is also a key parameter in the assessment against fracture. Herein, limit loads are usually estimated for defects in non-work-hardening materials [4-6]. A greater number of existing solutions for limit pressure of a cracked tube have been developed either analytically, based on a simple equilibrium stress field, or empirically, based on test data [4]. These solutions are generally shown to be too conservative for components with part-through-thickness defects. Recently, a finite element based plastic limit pressure expres-

---

[1]Faculty of Mechanical Engineering and Naval Architecture, Institute of Applied Mechanics, University of Zagreb, Zagreb, Croatia

sion for cylinders with external axial semi-elliptical surface cracks has been developed in Ref. [6]. However, the proposed expression is applicable to a very limited range of crack dimensions and therefore extended solutions are needed. Closed-form of plastic limit pressure solutions for a considered tube and crack geometries have not been presented in literature yet.

The objective of this work is to obtain a new solution for the stress intensity factor and plastic limit pressure for VVER steam generator tubes with external axial surface cracks, which are subjected to internal pressure, as shown in Fig. 1. These thick tubes are made of austenitic steel 08X18H10T that corresponds to AISI 321 grade [7]. Both linear and non-linear FE analyses have been performed. The FE solutions generated in this study have been used to develop the new stress intensity factor influence coefficients and the analytical approximation of the plastic limit pressure for a wide range of external axial semi-elliptical surface cracks in tubes.

Finite element analysis

Finite element analysis has been performed to evaluate plastic limit pressure, stress intensity factor and J-integral for a tube with an external axial surface crack subjected to internal pressure p. The tube geometry and loading are shown in Fig. 1. The outer radius of VVER tube R_0 is 8 mm and the wall thickness t is 1,5 mm (R_m/t=4.83). The crack is assumed to have a semi-elliptical shape described by a length $2c$, depth a and normalized crack length ρ, defined as $\rho = c / \sqrt{R_m t}$. Six different crack lengths were considered, $2c =$ 5, 10, 20, 30, 40 and 50 mm, and four values of the ratio of the crack depth to the tube thickness were selected, a/t = 0.2, 0.4, 0.6 and 0.8. The tube length ($2L$) was always chosen large enough so that the boundary would have a negligible effect on the fracture response characteristics ($L/c \geq 10$) [2]. As evident from Fig. 1, the internal pressure p is applied as a distributed load to the inner surface, together with an axial tension force P equivalent to the internal pressure applied at the end of the tube to simulate the closed end. Mechanical properties of the austenitic steel 08X18H10T are as follows [7]:

at 20 ^{0}C E=209 GPa, σ_Y = 250 MPa, σ_U = 560 MPa, α = 1.920, n = 4.59,

at 300 ^{0}C E=184 GPa, σ_Y = 160 MPa, σ_U = 420 MPa, α = 1.375, n = 4.01,

where E is Young's modulus, σ_Y is the yield stress and σ_U is the ultimate stress. The values α and n denote the parameters fitting experimentally the obtained curve. The solutions for elastoplastic J-integral values are obtained using the deformation theory of plasticity.

The finite element analysis is performed using the commercial FE package ABAQUS/Standard [8]. A typical finite element mesh used in the analysis is shown in Fig. 2. To avoid problems associated with incompressibility, 20-node brick elements (C3D20R) with reduced integration are used. Due to symmetry, only a quarter of the tube was modelled where the number of elements and nodes ranges from 2094 ele-

ments/10623 nodes to 8225 elements/39653 nodes. In order to model strain singularity at the crack tip correctly, collapsed wedge-shaped elements are applied. The crack-tip mesh refinement illustrating these focused elements is depicted in Fig. 2b. The values of the *J*-integral are computed around 5 contours surrounding the crack tip. The result from the 1st contour closest to the crack tip is discarded, and the *J*-integral value is the average of all the values obtained on the 2nd to 5th contours.
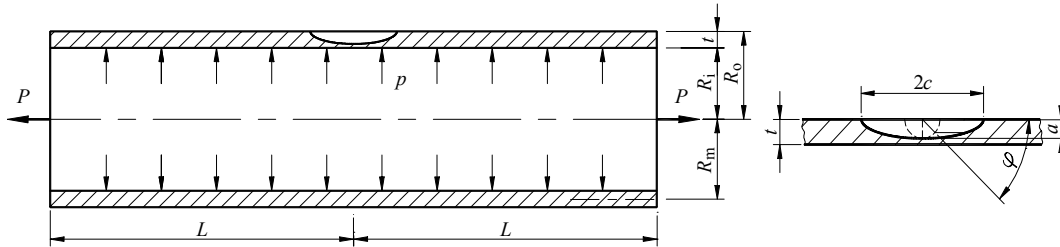
Figure 1: Geometry and dimensions of a tube subjected to internal pressure with an external axial semi-elliptical surface crack

(a)   (b)
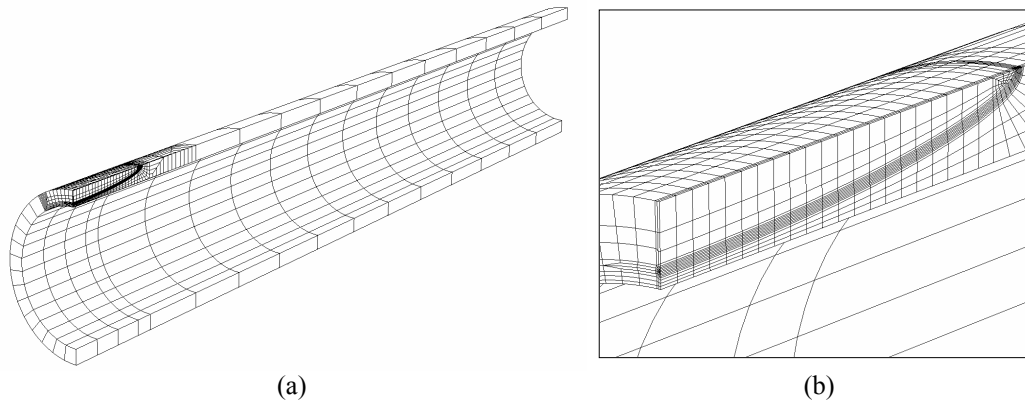
Figure 2: Typical FE mesh for a tube with external axial surface crack
(2*c* = 20 mm, *a/t* = 0.8): (a) whole mesh; (b) crack tip mesh

Stress intensity factor

The stress intensity factor *K* for an external axial surface crack in a tube under internal pressure may be expressed by the following relation [2]

$$K = \frac{p\,R_m}{t}\sqrt{\pi\,a}\;F\!\left(\frac{R_m}{t}, \frac{a}{t}, \rho, \varphi\right), \tag{1}$$

where $F(R_m/t, a/t, \rho, \varphi)$ is a dimensionless function depending on the tube and crack geometry and φ is the angle defining the crack front position (see Fig. 1). The values of function $F(a/t, c)$ obtained from the FE analysis for the considered tube geometry are

tabulated in Tables 1 and 2. As the SIF values reach the largest values at the deepest crack front location ($\varphi = \pi/2$), only the results at that location are given. The accuracy of SIFs calculated from the FE analysis is examined in Fig. 3. The values of the dimensionless function F for the stress intensity factor obtained by this study are compared with the solutions presented in Ref. [2] for the selected values of t/R_i=0.25, a/c=0.2, 0.4, 1.0 and a/t=0.2, 0.5, 0.8. The results compare satisfactorily, while only slight differences in less than 6% of the F values are exhibited. The differences occur due to the numerical inaccuracy of the Raju and Newman results [2], as also shown in Ref. [1].

Table 1: Dimensionless function F for the stress intensity factor ($2c$ = 5, 10 and 20 mm)

$2c$	5 mm				10 mm				20 mm			
a/t	0.2	0.4	0.6	0.8	0.2	0.4	0.6	0.8	0.2	0.4	0.6	0.8
F	0.992	1.125	1.204	1.184	1.039	1.331	1.680	1.967	1.060	1.451	2.045	2.797

Table 2: Dimensionless function F for the stress intensity factor ($2c$ = 30, 40 and 50 mm)

$2c$	30 mm				40 mm				50 mm			
a/t	0.25	0.4	0.6	0.8	0.2	0.4	0.6	0.8	0.2	0.4	0.6	0.8
F	1.150	1.492	2.173	3.129	-	1.516	2.240	3.279	-	1.530	2.282	3.376
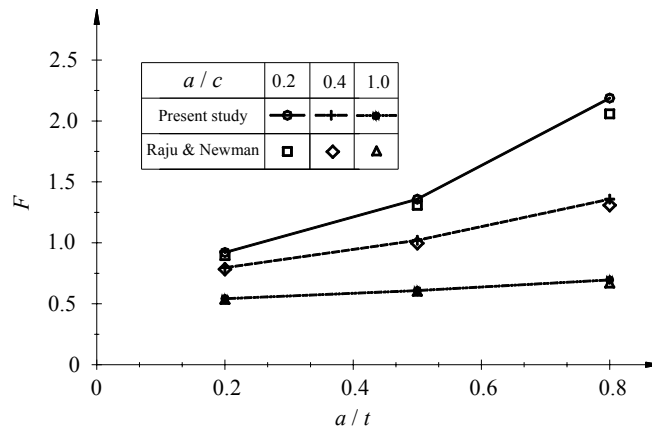
Figure 3: A comparison of dimensionless function F for the stress intensity factor K between the present work and the published solutions by Raju and Newman [2]

Plastic limit pressure

In the elastic–perfectly plastic FE limit load analysis the internal pressure load was applied incrementally using the RIKS algorithm within ABAQUS [8] until the collapse of

the tube was indicated. This gives the limit pressure p_L for a tube with an external axial surface crack. Based on the present FE results, the following empirical expression for the estimation of plastic limit pressure is derived in terms of non-dimensional crack configuration parameters a/t and ρ, as follows:

$$p_L = \frac{2}{\sqrt{3}} \sigma_Y \ln \frac{R_o}{R_i} \left[A_0 + A_1 \left(\frac{a}{t} \right) + A_2 \left(\frac{a}{t} \right)^2 \right], \tag{2}$$

where

$$A_0 = 1, \quad A_1 = 0.14089 - 0.39607\,\rho + 0.06902\,\rho^2 - 0.00415\,\rho^3,$$
$$A_2 = -0.10307 + 0.00347\,\rho - 0.00969\,\rho^2 + 0.00094\,\rho^3. \tag{3}$$

For the considered ranges, the proposed empirical relation predicts the limit pressure which differs less than 4% from the FE solutions. In the limit case of $a/t \rightarrow 0$, the above expression reduces to $p_L = 2/\sqrt{3}\,\sigma_Y \ln(R_0 / R_i)$, which is the fully plastic collapse pressure solution for an uncracked thick walled tube based on the Von Mises yield criterion [5]. Recently, Kim et al. [6] have proposed a similar equation for the plastic limit pressure based on selected FE limit analyses using the parameters R_m/t=20, ρ=0.5, 1.0, 2.0 and 3.0. Furthermore, the plastic limit pressures for the considered steam generator tube geometry obtained by the equation proposed by Kim et al. [6] are compared with the present FE results in Fig. 4. As may be seen, the FE results for the large crack length from this work are generally different from those from the Kim et al. [6] equation. This could be because the Kim et al. solutions are given only for limited ranges of tube and crack geometries.
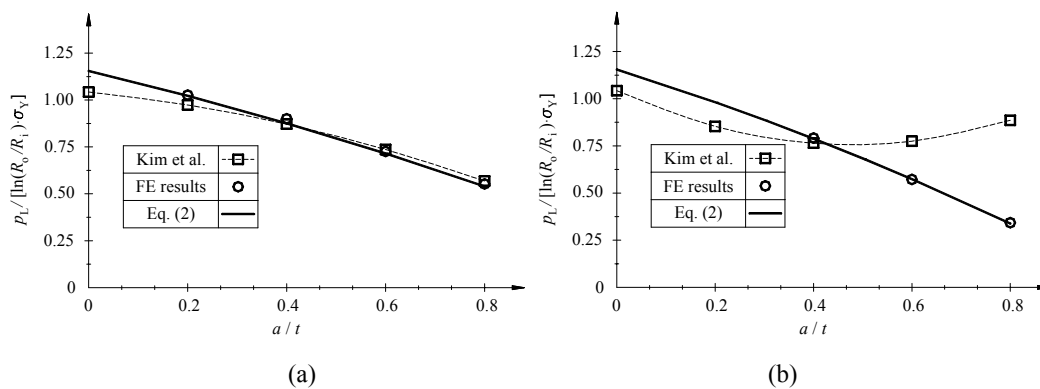
Figure 4: A comparison of plastic limit pressure p_L between the present work and the published solutions by Kim et al. [6]: (a) 2c=20 mm; (b) 2c=50 mm

Conclusion

Using the detailed non-linear finite element analyses, the stress intensity factors, the *J*-integral and the plastic limit loads for external axial semi-elliptical surface cracks in VVER steam generator tubes under internal pressure were computed. The results for the stress intensity factors are presented in terms of the well-known GE/EPRI influence functions and are compared with the Raju and Newman solutions. The plastic limit pressure solutions were obtained by the finite element limit analyses using elastic-perfectly plastic material behaviour. These solutions were used to develop a new analytical approximation of the plastic limit pressure, which is applicable to a wide range of crack dimensions.

The proposed SIFs and the analytical approximation of limit pressure for the considered geometries are very useful tools for assessing the integrity of pressurized tubes. Further investigations should be directed towards the determination of the plastic influence h_1-functions (GE/EPRI method) for the elastoplastic *J*-integral.

References

1   Kim, YJ., Kim, JS., Park, YJ. and Kim, YJ. (2004): "Elastic–plastic fracture mechanics method for finite internal axial surface cracks in cylinders", *Engineering Fracture Mechanics,* Vol. 71, pp. 925-944.

2   Raju, I.S. and Newman, J.C. (1982): "Stress-intensity factors for internal and external surface cracks in cylindrical vessels", *Journal of Pressure Vessel Technology,* Vol. 104, pp. 293–298.

3   Ainsworth, R.A. (1984): "The assessment of defects in structures of strain hardening material", *Engineering Fracture Mechanics,* Vol. 19, pp. 633–642.

4   Miller, A.G. (1988): "Review of limit loads of structures containing defects", *International Journal of Pressure Vessels and Piping*, Vol. 32, pp. 191–327.

5   Zarrabi, K., Zhang, H. and Nhim, K. (1997): "Plastic collapse pressure of cylindrical vessels containing longitudinal surface cracks", *Nuclear Engineering and Design,* Vol. 168, pp. 313-317.

6   Kim, YJ., Shim, DJ., Nikbin, K., Kim, YJ., Hwang, SS. and Kim, JS. (2003): "Finite element based plastic limit loads for cylinders with part-through surface cracks under combined loading", *International Journal of Pressure Vessels and Piping,* Vol. 80, pp. 527-540.

7   Timofeev, B.T., Karzov, G.P., Blumin, A.A. and Anikovsky, V.V. (1999): "Fracture toughness of austenitic welded joints", *International Journal of Pressure Vessels and Piping*, Vol. 76, pp. 393-400.

8   ABAQUS (2004) "*User's guide and theoretical manual*", Version 6.4, Hibbitt, Karlsson & Sorensen, Inc.